Photodegradation of Poly(*n*-butyl acrylate). Photochemical Processes in Polymeric Systems. 8†

Ranty H. Liang,* Fun-Dow Tsay, and Amitava Gupta*

Energy and Materials Research Section, Jet Propulsion Laboratory, California Institute of Technology, Pasadena, California 91109. *Received August 13, 1981*

ABSTRACT: The photochemistry of poly(*n*-butyl acrylate) (P*n*BA) has been studied at 77 and 298 K. The principal photoproducts of Norrish type I and II processes have been identified and their quantum yields have been measured. The chemistry of photogenerated radicals has been monitored via ESR spectroscopy. Both Norrish type I and II products are observed at room temperature on excitation at 253.7 nm. Hydrogen abstraction takes place from backbone methylene groups in samples excited at 77 K, while tertiary hydrogen abstraction from the main chain becomes the dominant radical termination process at or above 210 K, which is the glass transition temperature of P*n*BA. Excitation at 313 nm in the presence of air causes photooxidation but little or no photolytic bond cleavage.

Introduction

The photochemistry and photothermal degradation of poly(alkyl acrylates) have been studied mainly from two viewpoints: (1) effect of segmental mobility on the radical deactivation pathway and (2) reactivity of the excited ester chromophore.[2-7] The photochemistry of elastomeric polyacrylates may be controlled by the lifetime of the excited state. If it is much longer than the time required for segmental rotation, the excited ester group may gain access to abstractable hydrogen atoms on the main chain. Abstraction may then be followed by a Norrish type II deactivation of the biradical, affording a nonradical pathway to chain scission (Scheme I). This process was shown to be inefficient for poly(methyl acrylate) (PMA) at 25 °C by Fox et al.,[2] who measured scissions per polymer chain on exposure to 253.7-nm radiation in a vacuum and determined that it was close to zero at room temperature. However, in their study, they did not separately evaluate the effects of cross-linking and chain scission on viscosity. Little is known of the reactive excited state in poly(alkyl acrylates). Monahan[8] identified the major photoprocess in poly(*tert*-butyl acrylate) (P*t*BA) and proposed a rotational isomerization mechanism as the key step preceding a type II photoreduction of the ester carbonyl group. The observed photoreactivity in P*t*BA was assigned to the first $n\pi^*$ triplet state based on triplet quenching studies using triplet quenchers such as benzophenone and naphthalene.[9] Radical deactivation pathways have been inferred from an analysis of volatiles and also from relative rates of cross-linking and chain scission in poly(*n*-butyl acrylate).[4,6] In our work on poly(methyl methacrylate) (PMMA) photolysis[10] at room temperature, we determined that most macroradicals ultimately decay via recombination with small radicals such as $\cdot CH_3$ and $\cdot CHO$. Essentially the same conclusion was reached by Fox et al. on the basis of the total quantum yield of reaction measured for PMA.[2] Existence of a large alkyl side chain as in poly(*n*-butyl acrylate) (P*n*BA) would be expected to provide additional configurations for type II processes and also additional sites for cross-linking. In this respect, mention may also be made of a recent report by Rogers et al.[11] in which they described changes in infrared spectra and gel fraction of thin P*n*BA films on exposure to Pyrex-filtered radiation from a medium-pressure mercury arc lamp.

In this paper we report on the photochemical reactivity of the excited state of the ester chromophore in P*n*BA. The emission spectrum and lifetime of the lowest excited state have also been measured. ESR spectroscopy has been used to elucidate the initial hydrogen abstraction mechanism at 77 K, P*n*BA being in the glassy state at that temperature. The subsequent chemical evolution of these radicals generated at 77 K has been monitored, both in the presence and in the absence of oxygen. Work in progress with this system involves use of spin-trapping techniques to isolate transient radicals generated during photolysis and estimation of the quantum yield of the chain scission reaction.

Experimental Section

Sample Preparation. Poly(*n*-butyl acrylate) was synthesized via thermal polymerization by refluxing the monomer in cyclohexane under high-purity nitrogen gas for periods up to 48 h. The polymer was purified by dissolving the sample in dichloromethane and then reprecipitating it by adding methanol to the dichloromethane solution. The number-average molecular weight obtained, as measured by GPC (high pressure), was $\sim 8 \times 10^5$ (polystyrene calibration). The polymer was clear, transparent, and extremely tacky. Samples of P*n*BA were dissolved in dichloromethane and cast into thin films on various substrates. Quartz substrates were used for UV–visible spectroscopic analysis as well as gel content measurement and measurement of weight loss as a function of irradiation time. Films were cast on the inner surface of quartz ESR tubes for ESR spectroscopic analysis. Salt (KBr and NaCl) flats were used as substrates for FT IR analysis. These films were dried slowly to drive off the solvent and were subsequently vacuum pumped overnight before they were irradiated. Solvents for GPC and fluorescence analyses were purified by passing them through a basic alumina column followed by distillation.

Irradiation. Three sources of irradiation were used. A low-pressure mercury lamp (>99% intensity at 253.7 nm) was used as the source of radiation in most experiments at room temperature. A few room-temperature tests were performed with the isolated 313-nm mercury line in a medium-pressure Hg arc lamp. The fourth harmonic of a Nd:YAG laser (266 nm) was the source of irradiation for exposures at 77 K. The laser delivered 15 mJ per pulse, approximately 5×10^{14} photons being absorbed by the P*n*BA sample per pulse. Radiation flux at the sample plane was measured by performing actinometry, with *o*-nitrobenzaldehyde as an actinometer. The quantum yield of rearrangement of *o*-nitrobenzaldehyde was estimated to be 0.50 ± 0.03 at 253.7 nm.[12,13]

Quantum Yields. Samples were irradiated at room temperature in a sealed quartz tube with a break-seal in a side arm. After irradiation, the quartz tube was immersed in liquid nitrogen, and dichloromethane was introduced through the break-seal in a closed system to dissolve the volatile photoproducts. The solution was then allowed to warm to room temperature. It was analyzed by GC/MS to identify the photoproducts, while quantitative measurements were carried out by gas chromatographic analysis. Control runs with known added concentrations of photoproducts which were identified initially were also performed in order to verify that at these conversions, the photoproducts

†This paper represents one phase of research performed at the Jet Propulsion Laboratory sponsored by the National Aeronautics and Space Administration under Contract NAS7-100. This research was performed in support of the Low Cost Solar Array Project, Encapsulation Task, sponsored by the Department of Energy.

0024-9297/82/2215-0974$01.25/0

Scheme I

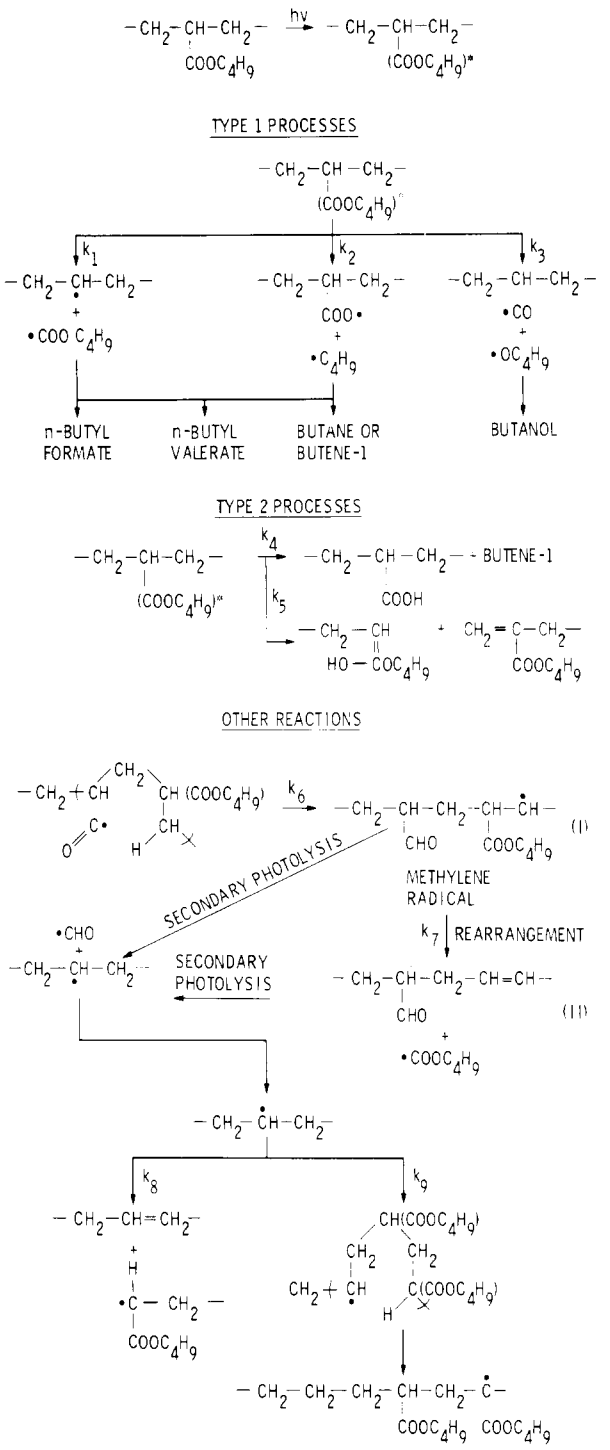

(including 1-butene) were completely extracted and solubilized by dichloromethane prior to GC/MS and GC analyses.

Spectroscopic Measurements. Electronic spectra were recorded on a Cary 219 spectrophotometer fitted with an integrating sphere. FT IR spectra were recorded on a Digilab 15C FT IR spectrometer. ESR spectra were recorded on a Varian E-Line Century Series spectrometer operating at X-band frequency (9.1–9.5 GHz) and employing 100-kHz field modulation. Absence of saturation was ensured by using 0.1–1.0-mW power to obtain the ESR spectra. Measurements were made on samples sealed in 3-mm-i.d. quartz tubes. The spectrometer was equipped with a Varian variable-temperature accessory. Temperature was measured with a calibrated copper vs. constantan thermocouple placed in the same cavity position as the sample. An on-line computer system (Varian Model No. 900 data acquisition system) was used to facilitate the spectral acquisition, data analysis, and intensity measurements. Samples were irradiated in sealed ESR

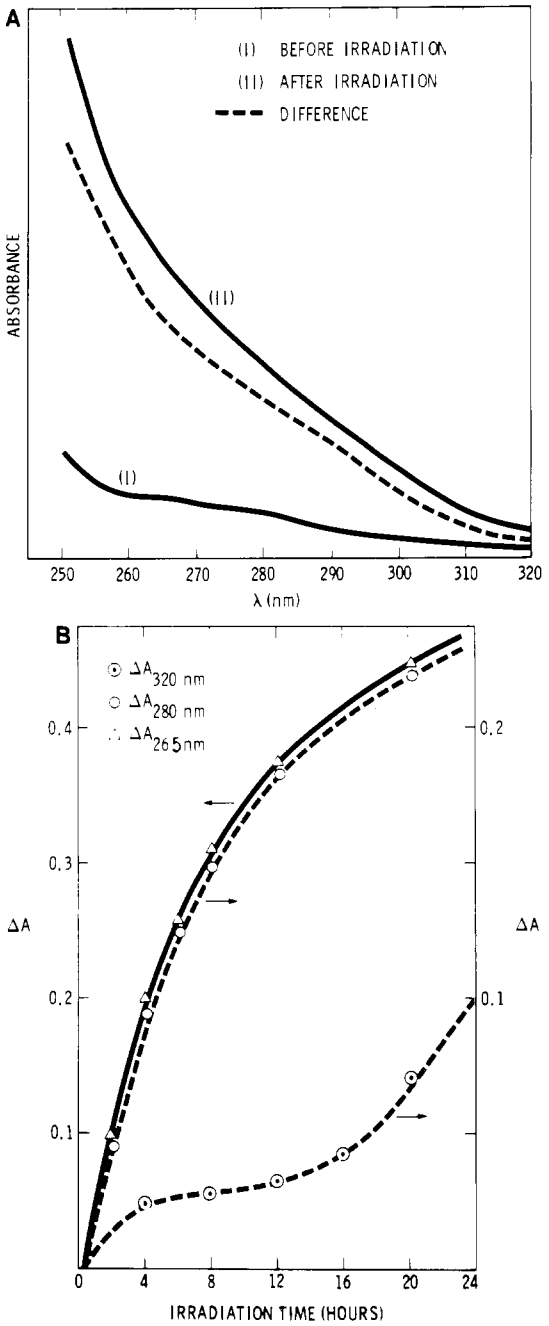

Figure 1. Changes in absorbance of PnBA films irradiated in air at 253.7 nm (30 °C).

quartz tubes at 77 K with the pulsed laser beam at 266 nm. The irradiated samples were then transferred to the ESR cavity for measurement at temperatures ranging from 77 to 300 K. Radical concentrations were measured by double integration of the first-derivative ESR curve and by comparison with a standard DPPH (diphenylpicrylhydrazyl) sample using the computer system.

Emission spectra were recorded on a Perkin-Elmer MPF-3A spectrofluorimeter. Both degassed and aerated solutions were investigated by using freshly distilled *trans*-1,3-pentadiene as a triplet quencher. Emission lifetime measurements were carried out by exciting the sample with the pulsed laser and collecting the emission on a fast-rise photodiode, the signal from which was directly monitored on a Tektronix scope.

Results

Figure 1A shows the absorption spectra of PnBA obtained before and after room-temperature irradiation in the presence of O_2, as well as the difference spectrum down to 250 nm. Figure 1B shows plots of ΔA_{265}, ΔA_{280}, and ΔA_{320} vs. irradiation time. While the absorbance increases

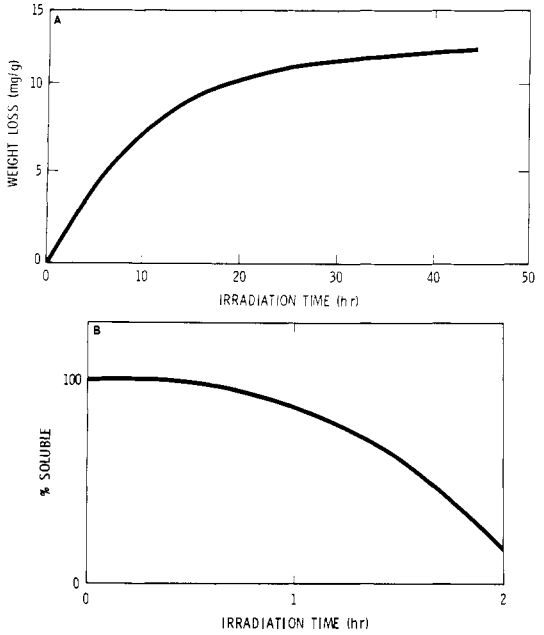

Figure 2. Physical changes in P*n*BA films on irradiation at 253.7 nm in air (30 °C): (A) weight loss vs. irradiation time; (B) sol fraction vs. irradiation time. Samples were initially un-cross-linked.

Table I
Quantum Yields of Photoproducts of P*n*BA Films

product	quantum yield
1-butene	0.1[a]
	<0.01[b]
butane	<0.01[a,c]
1-butanol	0.02[a]
n-butyl formate	0.03[a]
n-butyl valerate	~0.01[a]
total radical concn at 77 K	0.6[d]

[a] 253.7-nm irradiation under vacuum. [b] 313-nm irradiation under vacuum; no butene was detected. [c] No butane was detected. [d] 266-nm irradiation under vacuum.

monotonically at 265 and 280 nm, the increase in absorbance at 320 nm is found to have an induction period. The increase in absorbance at 265 and 280 nm may be attributed to the formation of primary photoproducts. These two curves subsequently level off, presumably due to competitive absorption of radiation by photoproducts. The rapid rise in absorbance at 320 nm after 2 h of irradiation (Figure 1B) may therefore be due to formation of products of photolysis of these initial photoproducts. Figure 2A shows a plot of weight loss of P*n*BA films as a function of irradiation time. This curve also levels off at approximately the same integrated radiation flux at which ΔA_{265} and ΔA_{280} level off, indicating that weight loss is caused by one of the primary photoprocesses presumably involving cleavage of the ester functionality. Figure 2B is a plot of the dichloromethane-soluble fraction of P*n*BA as a function of irradiation time. Apparently, P*n*BA undergoes cross-linking upon irradiation and becomes almost totally insoluble (>95%) in dichloromethane after 2 h of irradiation. Cross-linking of elastomeric acrylates had previously been observed by Fox[2] and also by Morimoto[4] in poly(methyl acrylate) and more recently by Rogers, Simha, and Dickinson[11] in P*n*BA. Table I gives the quantum yields of the major photoproducts. Among other low molecular weight species detected was *n*-butyl valerate, whose quantum yield of formation was less than 0.01. Figure 3

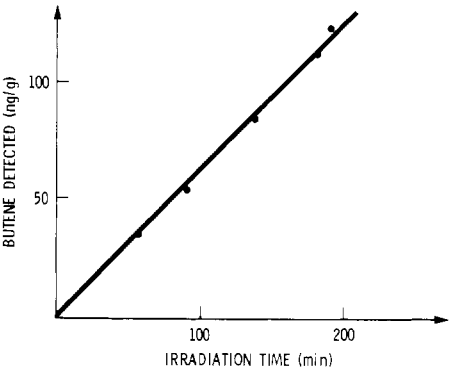

Figure 3. Yield of 1-butene as a function of irradiation time; P*n*BA films deposited on quartz flats were irradiated under vacuum at room temperature using 253.7-nm radiation.

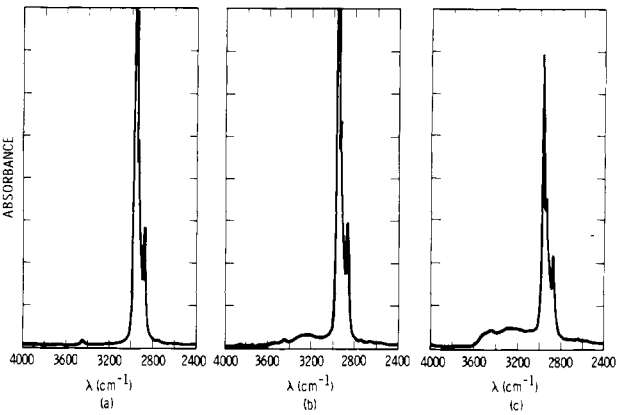

Figure 4. FT IR spectra of P*n*BA films deposited on salt flats irradiated at room temperature using 253.7-nm radiation: (a) before irradiation; (b) irradiated under vacuum; (c) irradiated in the presence of air.

is a plot of 1-butene formation with irradiation time, showing that the quantum yield measurements were made at low conversions.

FT IR spectra of the irradiated P*n*BA films (253.7 nm, in air as well as under vacuum) showed three common features when compared with spectra of control (unirradiated) films: (1) The C=O stretch (1725 cm^{-1} and overtone at 3450 cm^{-1}) lost intensity, indicating photochemical cleavage of the ester group; (2) a shoulder developed at 1780 cm^{-1}; and (3) a peak at 3260 cm^{-1} was formed as a result of formation of hydroxyl groups (Figure 4b).

However, when P*n*BA films were irradiated in air, an additional hydroxyl peak appeared at 3480 cm^{-1} as shown in Figure 4c. FT IR spectra were recorded separately on both the dichloromethane-soluble and -insoluble components of a sample irradiated in air. The peak at 3260 cm^{-1} was found to be associated with the soluble component while the 3480-cm^{-1} peak was present in the insoluble component; hence the latter peak is assigned to a hydroxyl group bound to the network which undergoes cross-linking and thus becomes insoluble in dichloromethane.

ESR spectra of P*n*BA irradiated at 77 K in the absence of oxygen are shown in Figure 5. These spectra were recorded as a function of temperature as the irradiated samples were gradually warmed to room temperature inside the ESR cavity. Spectra at 77 K were complicated, but the presence of a doublet with a hyperfine splitting of 126 G was unmistakable after 400 laser pulses. This spectrum could be resolved into five components (Figure 6): a sextet, a quartet, a broad singlet, a relatively sharp singlet, and the doublet mentioned above, which could be assigned to ·CHO. The simulation was performed for the

Table II
ESR Parameters of Radicals Generated from Laser-Irradiated PnBA at 77 K

radical	spectral feature and line width ΔH	g values	proton hyperfine coupling constants, G	rel intens[a]
$CH_2CH(C\dot{O})CH_2$ and/or $\cdot COOC_4H_9$	narrow singlet, ΔH = 13 G	2.002 ∓ 0.001		0.33
$CH_2CH(C\dot{O}O)CH_2$ and/or $\cdot OC_4H_9$	broad singlet, ΔH = 30 G	2.002 ∓ 0.001		0.14
$CH_2\dot{C}HCH_2$	sextet, ΔH = 14 G	2.002 ∓ 0.001	21.0 ∓ 1.0	0.34
$CH(COOR)\dot{C}HCH(COOR)$	quartet, ΔH = 13 G	2.002 ∓ 0.001	22.0 ∓ 1.0	0.16
$\cdot CHO$	doublet, ΔH = 10 G	2.003 ∓ 0.001	126.0 ∓ 2.0	0.03

[a] At 1000 laser pulses.

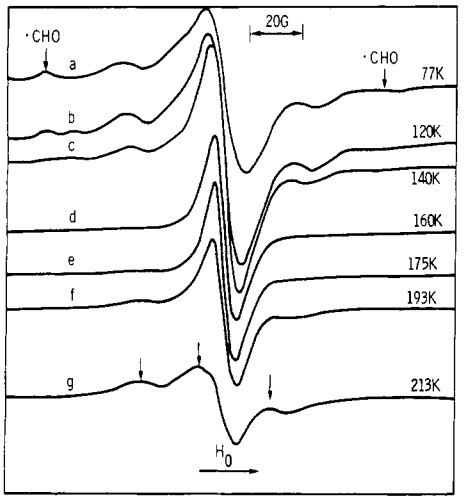

Figure 5. ESR spectra of PnBA samples irradiated at 77 K under vacuum using the fourth harmonic of the Nd:YAG laser (266 nm). Radio-frequency power level, 10 mW; laser pulses accumulated, ~1000 pulses. The sample was gradually warmed in the cavity, and spectra were recorded at the specified temperatures.

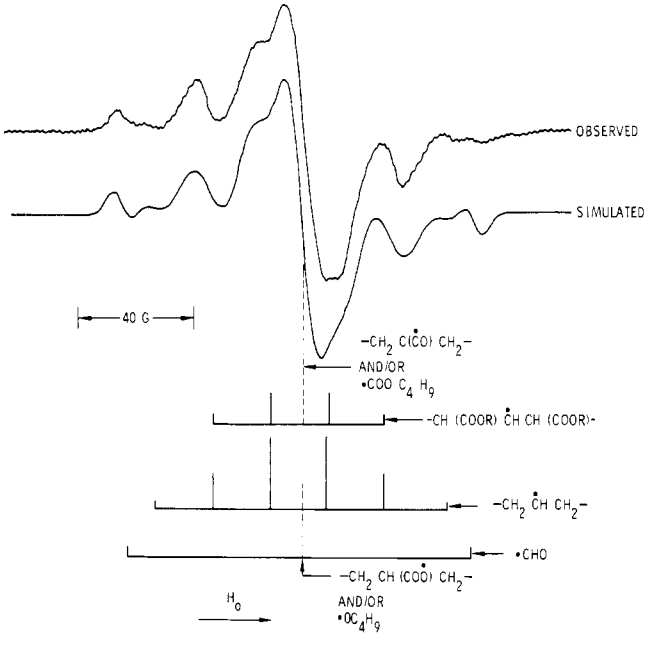

Figure 6. Computer simulation of the 77 K ESR spectrum of PnBA samples irradiated at 77 K under vacuum. Accumulated dosage, ≃1000 laser pulses. Radio-frequency power level, 1.0 mW. For details of spectral components simulated, see Table II.

spectrum recorded on a frozen sample irradiated with 1000 laser pulses (see Discussion). At low fluxes, the amplitude of the broad singlet was approximately twice that of the narrow singlet component. As the sample irradiated under vacuum was warmed to 140 K, a singlet appeared in the

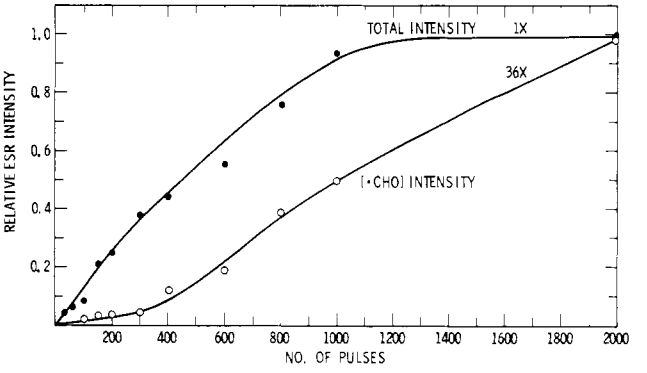

Figure 7. Radical concentration measured as a function of accumulated laser power dosage. Samples were irradiated at 77 K under vacuum and absorbed ~5 × 10^{14} photons per pulse.

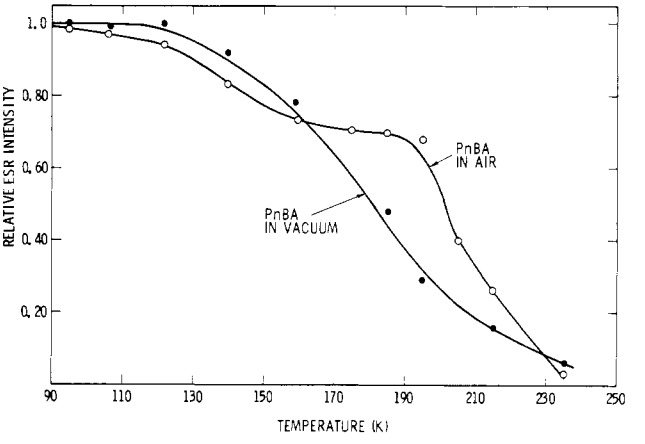

Figure 8. Total radical concentration vs. temperature as measured by ESR spectroscopy on sealed samples irradiated at 77 K under vacuum and in the presence of air. Radio-frequency power level, 1.0 mW.

ESR spectrum (Figure 5c). Upon further warming to 213 K (Figure 5g) the singlet evolved into a triplet with a hyperfine coupling constant of 25 G, which eventually decayed at room temperature. Figure 7 shows plots of total radical concentration as well as the ·CHO radical concentration vs. the total laser flux used to irradiate the sample at 77 K. The total radical concentration leveled off after 1000 laser pulses, while ·CHO concentration became appreciable only after 400 pulses, demonstrating that the formation of ·CHO involved secondary photolysis. Figure 8 shows a plot of the total concentration of radicals as a function of temperature. The total concentration remained constant up to 130 K, above which there was a gradual decrease.

Relative yields and coupling constants of all radical species are given in Table II. Figure 9 shows ESR spectra of samples irradiated at 77 K in the presence of oxygen. The 77 K spectrum is quite similar to that of the sample

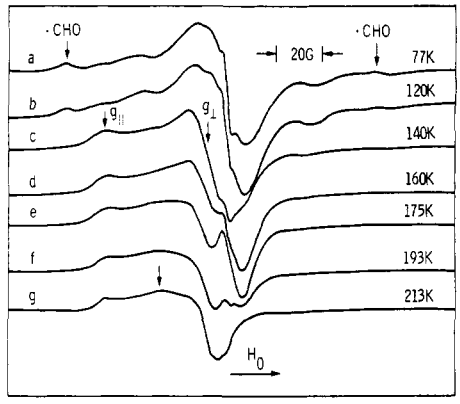

Figure 9. ESR spectra of P*n*BA films irradiated in the presence of oxygen at 77 K using the fourth harmonic of the Nd:YAG laser (266 nm). Radio-frequency power level, 10 mW; laser pulses accumulated, ~1000 pulses. The sample was gradually warmed in the cavity, and spectra were recorded at the specified temperatures.

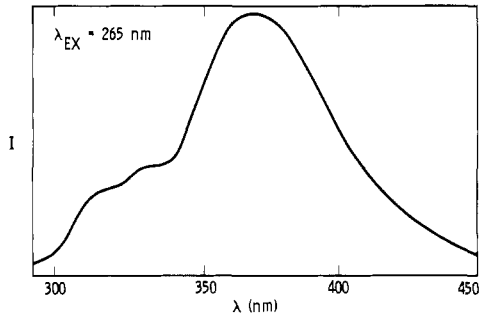

Figure 10. Uncorrected emission spectrum of P*n*BA in CH_2Cl_2 solution at 30 °C. λ_{ex} = 265 nm.

irradiated under vacuum. As the sample irradiated in air was warmed to 140 K, its ESR spectrum (Figure 9c) was dominated by signals from peroxy radicals with characteristic anisotropic g values ($g_{\perp}$ = 2.007, $g_{\parallel}$ = 2.034). These radicals appeared to be bound to the main chain, since they had a broad line shape characteristic of a polymeric radical in a rigid glassy matrix. Peroxy radicals on side chains are unlikely to produce this line shape, because side-chain motion is not entirely suppressed in P*n*BA at 140 K, and hence, signals from a radical center on the *n*-butyl side chain would be motionally narrowed at 140 K. Again, a singlet appeared at 170 K (Figure 9e) over and above the intense peroxy radical signal.

Figure 10 shows the uncorrected emission spectrum of P*n*BA in fluid dichloromethane solution. Time-resolved experiments indicated that the emission lifetime is less than 20 ns, which is the limit of resolution in this apparatus. The emission was readily quenched by *trans*-1,3-pentadiene. Stern–Volmer treatment of the quenching data yielded an excited-state lifetime of approximately 10 ns, assuming a diffusion-controlled quenching rate constant.

Discussion

The quantum yields of formation of all species are given in Table I, while the relative yields of all radicals are given in Table II. Infrared spectra and sol–gel analysis provide evidence for additional photoprocesses. In particular, analysis of the IR spectra of samples irradiated under vacuum shows that hydroxyl groups are being formed only as a substituent on a species which can be extracted, i.e., a low molecular weight species. This is identified as 1-butanol. IR spectra of samples irradiated in air show that in addition to 1-butanol, a hydroxyl group bound to the main chain is also being formed. This is presumably the main product of photooxidation at the tertiary hydrogen sites of the main chain. Scheme I described all of the principal photoprocesses which might be expected to occur on excitation of the ester chromophore in P*n*BA.

In the following discussion we have attempted to correlate the radicals detected by ESR spectroscopic analysis to products detected on photolysis at room temperature. This correlation tends to ignore the activation effects on the relative rates of competing processes. This can be avoided ultimately only by performing time-resolved ESR spectroscopy at room temperature at a sufficiently high resolution in order to obtain data comparable to what was obtained by photolyzing at 77 K. Another possible source of error is that the data in Table II were obtained after 1000 laser pulses were accumulated; hence they may not be entirely representative of primary photochemical processes.

Assignment of ESR Signals. The 120 K ESR spectrum of the sample irradiated under vacuum (Figure 5b) is dominated by a singlet, which may be assigned to the radicals $\cdot COOC_4H_9$ and/or $CH_2\dot{C}H(CO)$ formed by processes 1 and 3, respectively (Scheme I). When this singlet is subtracted from the 77 K spectrum, a sextet and a quartet remain along with a weak broad singlet and the doublet assigned to ·CHO. The computer-simulated spectrum and the 77 K spectrum recorded at 1000 laser pulses are illustrated in Figure 6. The simulated spectrum was obtained by varying the relative intensity and intrinsic line width of individual radical species to best fit the observed spectrum. All of the parameters used in the simulated spectrum are listed in Table II. The sextet can be assigned to $CH_2\dot{C}HCH_2$ (see Scheme I), which was observed by Rånby et al. as a product of radiolysis of polyethylene.[15] The quartet may be assigned to $CH(COOR)\dot{C}HCH(COOR)$,[16] presumably formed via hydrogen abstraction by an excited ester carbonyl group from a backbone methylene group (Scheme I, eq 6). No evidence for the presence of $CH_2\dot{C}H(COOC_4H_9)$ could be found in these samples, indicating that process 8 (Scheme I) is slow in P*n*BA at these temperatures. Consistent with this finding, no monomer (*n*-butyl acrylate), which would be expected to be formed on unzipping of this radical, could be detected in samples irradiated at room temperature. Possible deactivation routes for the radical $CH_2\dot{C}HCH_2$ are proposed in Scheme I, eq 9, which could result in the formation of the tertiary radical $CH_2\dot{C}(COOR)CH_2$. The broad singlet component may be assigned to the macroester or the butoxy radical formed via processes 2 and 3, respectively. It may be noted that the triplet (coupling constant 25 G), assigned to the main-chain tertiary radical $CH_2\dot{C}(COOR)CH_2$,[17] appears only at or above 210 K (Figure 5g), the glass transition temperature of P*n*BA. Spectral subtraction indicated that this radical could not constitute more than 5% of the radical population below 140 K, indicating that tertiary hydrogen abstraction begins to dominate as a radical deactivation pathway only at or just below T_g in this polymer. Below T_g, the major hydrogen abstraction mode appears to involve the methylene group, as shown in Scheme I, eq 6. The amplitude of the triplet signal is found to drop quite rapidly at or above T_g. This depletion is undoubtedly due to cross-linking processes, since small radicals (e.g., $\cdot COOC_4H_9$) are depleted by recombination processes below 210 K.

Scheme I also rationalizes the formation of ·CHO as products of secondary photolysis at 77 K, since I or II or a product thereof may absorb 266-nm radiation and yield CHO radicals.

The hypothesis that a secondary hydrogen abstraction is preferred to a tertiary hydrogen abstraction is not unreasonable if one considers the following:

1. At 77 K, the polymer or the chain radical does not have any appreciable segmental mobility. Preformed geometric configurations, therefore, provide the only opportunity for hydrogen abstraction. As illustrated in Scheme I, a six-member ring formation could only result in methylene hydrogen abstraction. Abstraction of tertiary hydrogens on the main chain requires prior formation of a more strained five-member ring.

2. The methylene hydrogens may be sterically more accessible than the main tertiary hydrogens on the main chain.

Figure 8 illustrates that while new radicals are formed when the vacuum-irradiated sample is warmed from 77 to 130 K, total radical concentration remains unchanged, implying that radical–radical recombination is not a major deactivation pathway in this temperature range. Therefore, the singlet observed at 140 K (Figure 5c) must evolve from the original radicals that exist at 77 K. The assignment of this singlet, which occurs in the ESR spectra in the temperature range 140–170 K, is not straightforward. Its narrow line width precludes any assignment to an oxygen radical. A likely candidate is $\cdot COOC_4H_9$, which may be readily formed from the methylene radical (eq 7, Scheme I).

The temperature evolution of the radicals generated at 77 K observed by us bears an approximate correspondence to that reported by Geuskens and David on poly(methyl acrylate).[18] The substantive difference is that we observe a broad triplet at or above T_g, which leads to its assignment to the main-chain radical $CH_2\dot{C}(COOR)CH_2$, assuming that the radical is present in several randomly distributed steric configurations.

Type II processes or hydrogen abstraction reactions requiring a cyclic transition state may be expected to be quite efficient at temperatures near or above the glass transition temperature but would be expected to take place at 77 K only if "preformed" transition state like configurations existed in the frozen polymer matrix. Thus our finding that abstraction of methylene hydrogens is quite efficient at 77 K may be useful in determining the thermodynamically preferred chain packing arrangement in this system below T_g.

Type I Quantum Yield Estimations. The total yield of the products of type I process may now be estimated from Table II and Scheme I as follows: six radical species can be formed as a result of type I cleavage (eq 1–3, Scheme I). Of the relative intensities of the six species (Table II), there is an approximate correspondence between the yield of the small ester radical $\cdot COOC_4H_9$ (narrow singlet) and $CH_2\dot{C}HCH_2$ (sextet). Therefore, it may be assumed that all of the macroacyl radicals, $CH_2CH(\dot{C}O)CH_2$, produced via process 3 (Scheme I) decay at 77 K via abstraction of main-chain methylene protons (eq 6, Scheme I), since the total relative yield of all radicals expected to produce the narrow singlet signal observed in 77 K cannot be more than 0.34. The yield of the secondary carbon radical $CH(COOR)\dot{C}HCH(COOR)$ formed via abstraction of methylene protons should then correspond to the initial yield of the macroacyl radicals (0.16). This type I cleavage (eq 3, Scheme I) causing the formation of macroacyl radicals should result in an equivalent yield of butoxy radicals, which is thus estimated to be 0.16 ± 0.02. The broad singlet is therefore seen to be entirely due to butoxy radicals, and yields of macroester radicals, $CH_2CH(COO\dot{)}CH_2$, and hence also butyl radicals, CH_3-$CH_2CH_2CH_2\cdot$ (eq 2, Scheme I), should be negligible. Hence the type I cleavage resulting in the formation of butyl radicals is not efficient at 77 K nor at room temperature, since no butane is detected. All of the 1-butene obtained is therefore produced by type II processes. Since the quantum yield of all radicals formed at 77 K was measured to be 0.6 (Table I), the total type I quantum yield may be estimated to be 0.3 at this temperature. Table III provides all quantum yield data measured for this system.

Scheme II

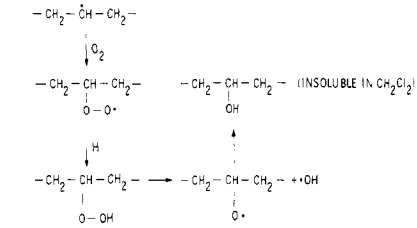

Table III
Quantum Yields of All Primary Photoprocesses

process	quantum yield
type I products: $\cdot COOC_4H_9$ and $CH_2\dot{C}HCH_2$	0.20 ± 0.02
type I products: $\cdot OC_4H_9$ and $CH_2CH(\dot{C}O)CH_2$	0.10 ± 0.01
type II products: 1-butene and $CH_2CH(COOH)CH_2$	0.1 ± 0.01

Photooxidation. When PnBA is exposed to 253.7-nm radiation in air, FT IR data indicate hydroxyl formation along the polymer main chain. Further evidence of oxygen insertion on the backbone comes from ESR data (Figure 9). Identical ESR spectra were obtained at 77 K for PnBA irradiated under vacuum and in air. At 140 K, however, peroxy radicals began to dominate the ESR spectrum. This might be due to an additional reaction taking place on diffusion of oxygen into the polymer matrix (Scheme II). The separation of $g_\perp$ and $g_\parallel$ as well as the broadened appearance of the ESR spectrum did not vary as a function of temperature in the range 140–170 K. This leads to the proposal that these peroxy radicals were bound to the main polymer chain, the formation of which may be interpreted in terms of the mechanism shown in Scheme II. It might be noted that the sharp singlet observed in samples irradiated under vacuum also appeared when the sample irradiated in air was warmed to 170 K (Figure 9).

When PnBA was exposed to 313-nm radiation in air, photooxidation took place as evidenced by the formation of hydroxyl groups. However, no butene or butanol could be detected when PnBA films were exposed to 313-nm radiation in air. These results might be interpreted by proposing that 313-nm radiation did not cause excitation of the ester group but resulted in photodissociation of main-chain hydroperoxy groups. The excitation of hydroperoxy groups might be direct or be caused by electronic energy transfer from main-chain carbonyl groups[19] whose presence was indicated by the phosphorescence spectrum of PnBA.

The plot of total radical concentration as a function of temperature (Figure 8) shows that radical recombination under vacuum occurred in the temperature range at which the β relaxation process is observed in this polymer. In the presence of oxygen, the temperature-dependent decay is the same as in evacuated samples, until a temperature was reached at which diffusion of oxygen caused transformation of most chain radicals to peroxy radicals. Decay of peroxy radicals (presumably via cross-linking) requires

segmental mobility and was hence observed to occur in the same temperature range as the glass transition process. This observation is consistent with the notion that most macroradicals generated on photolysis under vacuum ultimately decay via recombination with small radicals and also radical sites on side chains. Cross-linking is a much slower process and becomes an important pathway of radical deactivation only at a higher temperature or when photooxidation is carried out at 313 nm, causing photodissociation of main-chain hydroperoxy groups.

Acknowledgment. We thank Dr. D. Coulter for assistance in absorption measurements and A. Clayton in sample preparation. JPL Analytical Group support is also acknowledged. This paper is dedicated to Professor George Hammond for his pioneering research in the area of organic photochemistry.

References and Notes

(1) For Part 7, see: Gupta, M.; Gupta, A. *Polym. Photochem.*, accepted for publication.
(2) Fox, R. B.; Isaacs, L. G.; Stokes, S.; Kagarise, R. E. *J. Polym. Sci., Part A-1* **1964**, *2*, 2085.
(3) Phillips, D. *Photochemistry* **1976**, *7*, 505 and references therein.
(4) Morimoto, A.; Takamitsu, I. *Prog. Org. Coat.* **1973**, *1*, 35.
(5) Grassie, N.; Torrance, B. J. D.; Colford, J. G. *J. Polym. Sci., Part A-1* **1969**, *7*, 1425.
(6) Fourie, J.; McGill, W. *S. Afr. J. Chem.* **1979**, *32*, 156.
(7) McNeill, I. C.; Ackerman, L.; Gupta, S. N.; Zulfiguer, M.; Zulfiguer, S. *J. Polym. Sci., Polym. Chem. Ed.* **1977**, *15*, 2381.
(8) Monahan, A. R. *J. Polym. Sci., Part A-1* **1966**, *4* (10), 2381.
(9) Monahan, A. R. *J. Polym. Sci., Part A-1* **1967**, *5* (9), 2333.
(10) Gupta, A.; Liang, R.; Tsay, F. D.; Moacanin, J. *Macromolecules* **1980**, *13*, 1696.
(11) Rogers, C. E.; Simha, R.; Dickinson, H., private communication.
(12) Cowell, G. W.; Pitts, J. N., Jr. *J. Am. Chem. Soc.* **1968**, *90*, 1106.
(13) Gupta, A.; Yavrouian, A.; Di Stefano, S.; Merritt, C. D.; Scott, G. W. *Macromolecules* **1980**, *13*, 821.
(14) Ausloos, P. *Can. J. Chem.* **1958**, *36*, 383. Wijnen, M. H. J. *J. Chem. Phys.* **1958**, *28*, 939. *Can. J. Chem.* **1958**, *36*, 69.
(15) Rabek, J. F.; Skowronski, T. A.; Rånby, B. *Polymer* **1980**, *21*, 226.
(16) Browing, H. L.; Hazel, Jr.; Ackermann, D.; Patton, H. W. *J. Polym. Sci., Part A-1* **1966**, *4*, 1433.
(17) Szocs, F.; Rostasova, O. *J. Appl. Polym. Sci.* **1974**, *18*, 2529.
(18) Geuskens, G.; David, C. *Makromol. Chem.* **1973**, *165*, 273.
(19) Ng, H. C.; Guillet, J. E. *Macromolecules* **1978**, *11*, 929.

Photoprocesses in Copolymers of Methacrylophenone with Methyl Methacrylate: Photodegradation and Intramolecular Energy Migration

Toomas Kilp*

Radiation Laboratory, University of Notre Dame, Notre Dame, Indiana 46556

James E. Guillet

Department of Chemistry, University of Toronto, Toronto, Canada M5S 1A1

J. C. Galin and R. Roussel

Centre de Recherches sur les Macromolécules (CNRS), 67083 Strasbourg Cedex, France.
Received November 3, 1981

ABSTRACT: A series of poly(methyl methacrylate-*co*-methacrylophenone) copolymers were photolyzed in fluid solution with 313-nm radiation. Apparent quantum yields of degradation increased from 0.001 to 0.083 as the ketone content of the copolymers increased from 1.0 to 37.7 mol %. The magnitudes of these quantum yields are considerably lower than those previously reported for other methyl methacrylate–ketone copolymers. The depolarization of phosphorescence following excitation with plane-polarized light in 77 K solid solutions was measured as a function of copolymer composition. Results indicate that intramolecular energy transfer is a facile process in these systems. Migration of the excitation energy seems to be more dependent upon non-nearest-neighbor contacts between the ketone units than upon their presence in either dyad or triad sequences.

Introduction

Previous studies of the photolysis of ketone copolymers characterized by an absence of hydrogen atoms γ to the carbonyl have yielded interesting and often contradictory results. For example, Amerik and Guillet[1] have found the quantum yield of main-chain scission in fluid solution to rise from a value of 0.04 in the homopolymer of methyl vinyl ketone to a value of about 0.20 in its copolymer with methyl methacrylate. Photolysis of the copolymer in the solid state at temperatures above its glass transition has been shown by Dan and Guillet[2] to result in quantum yields similar to those obtained in fluid solution. Kato and Yoneshige[3] have found that the copolymer of acrylophenone with α-methylstyrene degrades much more slowly than does its copolymer with styrene. This behavior, which is attributable to a lack of abstractable γ hydrogens in the former case, was contradicted by their results of the photolysis of methyl vinyl ketone and acrylophenone copolymers with methyl methacrylate. The rapid degradation observed for these copolymers was unexpected in view of the lack of γ-hydrogen atoms. On the other hand, Lukac et al.[4] have found the quantum yield for main-chain scission of poly(acrylophenone) to be roughly halved when the ketone is copolymerized with methyl methacrylate.

Recently, Galin et al.[5] reported the first successful copolymerization of methyl methacrylate with methacrylophenone via a free radical mechanism. In view of the results cited above, it was felt that an investigation of some of the photoprocesses undergone by these copolymers would prove to be of interest.

Experimental Section

Photolysis of the poly(methyl methacrylate-*co*-methacrylophenone), PMMA–MAP, copolymers in toluene solution at 32 °C was carried out with 313-nm radiation from a medium-pressure mercury arc lamp. A Schott narrow-band interference filter (JENA UV-PIL) was used to isolate the desired wavelength from

0024-9297/82/2215-0980$01.25/0